

Performance investigation of metal hydride based heat transformer

Manoj Choudhari | Kunal Ahuja | Siddhant Thakkur | Subhro Bardhan |
Vinod Kumar Sharma 

School of Mechanical Engineering, Vellore
Institute of Technology, Vellore, India

Correspondence

Vinod Kumar Sharma, School of
Mechanical Engineering, Vellore Institute of
Technology, Vellore-632014, India.
Email: vinsharma85@gmail.com;
vinod_10_85@yahoo.com

Abstract

Energy is one of the major inputs for the economic development of any country. However, for developing countries energy is essential for economic growth, which calls for the development of clean and sustainable energy source/carrier. Among all the possible options, hydrogen has been considered as a promising clean energy carrier, which is associated with major challenges of its storage and application. Hydrogen can be stored safely in the form of metal hydrides whose formation and decomposition involve high heat interaction, which can be used for the development of thermodynamic systems like sorption heat pumps, which can transform waste heat to useful high-grade heat. In the present work, the performance of metal hydride based heat transformer (MHHT) is investigated in terms of variation in MH bed temperature and hydrogen interaction between coupled reactors during hydrogen transfer processes, in addition to thermodynamic performance (ie, Coefficient of Performance (COP), heating capacity, and so on) for the operating temperature of $T_L = 303$ K, $T_M = 383$ K, and $T_H = 423$ K. A pair of $\text{La}_{0.9}\text{Ce}_{0.1}\text{Ni}_5$ and $\text{LaNi}_{4.6}\text{Al}_{0.4}$ is chosen for present study based on author's previous work. In the present study, user-defined functions are employed in ANSYS Fluent, which consist of pressure, mass, and energy variation equations. The results are derived in the form of contours and graphical representations of variations in bed temperature and hydrogen concentration. It is observed that the system produces 40 kJ of upgraded heat with heating capacity of 0.1 kW and COP of 0.46 at 880 seconds of hydrogen transfer time for 250 g of each alloys.

KEYWORDS

ANSYS Fluent, CFD, metal hydride based heat transformer, metal hydrides, thermodynamic properties

1 | INTRODUCTION

Recently, Vinod and Anil^{1,2} gave a general idea about metal hydrides that is, its production, classification, and characterization. The review article also provides an exposure on how metal hydrides can be used for various thermodynamic applications including metal hydride based heat transformer

for waste heat recovery. With the increasing trend of renewable power and environment conservation, such projects show a very positive growth.

Several researchers³⁻⁶ have carried out their studies for the selection of best metal hydride pair for the optimum working of MHHT. Balakumar et al³ performed thermodynamic analyses of metal hydride based heat pumps and heat

transformers using different alloy pairs to facilitate the selection of pairs for particular application. Da-Wen et al⁴ reported that a two stage MHHT has a better potential than a single-stage MHHT. The study presents a method for selection of suitable alloys for two stage MHHT using following criteria: COP, alloy output, and temperature output. Ram Gopal and Srinivasa Murthy⁵ predicted the performance of the MHHT based on heat transfer and reaction kinetics employing ZrCrFe_{1.4}/LaNi₅ pair. Results showed that the performance of the system initially depends on heat transfer and eventually, as overall heat transfer coefficient exceeds a certain value, system performance dependence shifts to reaction kinetics. The performance improves as the output and heat rejection temperature decreases.

Several studies⁷⁻¹³ on the performance analyses of sorption thermodynamic systems are conducted using different MH pairs. Kang and Yabe¹² gave attention to metal hydride heat transformers for the effective use of industrial waste heat. Results showed that COP and heating output are increased as the waste heat temperature is increased. Moreover, the system performance can be enhanced with rectifications in reactor designs. Yang et al⁷ employed LaNi₅/LaNi_{4.7}Al_{0.3} pair for MHHT and performance was investigated using ambient and waste heat sources through two-dimensional unsteady model solved by finite volume method. Yang et al⁸ tried to account the realistic application for which they introduced a new dynamic index called true temperature boost for better assessment. Also, authors have developed mathematical models to deduce the appropriate results. Satya Sekhar and Muthukumar⁹ presented a thermal model for the performance of a MHHT using LaNi_{4.7}Al_{0.3}/LaNi₅ pair. Satya Sekhar et al¹⁰ presented numerical studies on MHHT and built a prototype for testing LaNi₅/LaNi_{4.35}Al_{0.65} pair. Satya Sekhar and Muthukumar¹¹ presented a detailed performance study of a MHHT working with three different alloy pairs: LaNi_{4.6}Al_{0.4}/MmNi_{4.15}Fe_{0.85}, LaNi_{4.61}Mn_{0.26}Al_{0.13}/La_{0.6}Y_{0.4}Ni_{4.8}Mn_{0.2}, and Zr_{0.9}Ti_{0.1}Cr_{0.9}Fe_{1.1}/Zr_{0.9}Ti_{0.1}Cr_{0.6}Fe_{1.4}. Kuznetsov¹³ presented with an investigation of working cycle of a MHHT for upgrading waste heat. Authors have also proposed a mathematical model for heat and mass transfer process in MHHT.

Some researchers¹⁴⁻¹⁷ performed studies on performance evaluation of two-stage MHHT. Werner and Groll¹⁴ developed a laboratory model for a two-stage metal hydride heat transformer. Three different misch metal-nickel-type alloys are used, with a limited maximum output of 135°C. Willers and Groll¹⁵ emphasized that out of all thermodynamic applications of metal hydrides, heat transformers, and heat pumps/refrigerator are most fascinating. The author's work gives an overview of an experimental setup provided with input heat of 130-135°C. Satya Sekhar and Muthukumar¹⁶ conducted various tests on a two stage MHHT and presented a prototype for further testing. La_{0.35}Ce_{0.45}Ca_{0.2}Ni_{4.95}Al_{0.05}/

LaNi₅/LaNi_{4.35}Al_{0.65} combination of alloy was used to study various parameters of performance for an input heat of 393 to 413 K. Satya Sekhar and Muthukumar¹⁷ presented a 2D thermal model of a two stage MHHT working with LaNi_{4.7}Al_{0.3}/LaNi₅/MmNi_{4.6}Al_{0.4} (low/medium/high pressure metal alloy) alloys combination. Predictions are made based on solution from solving heat and mass transfer equation. Also, the temperature variation for heat transfer fluid is presented over a cycle alongside the performance study for various parameters.

It is observed from the literature that metal hydride based heat transformers are good and efficient thermal system, which can able to upgrade waste heat (industrial waste heat, solar heat, and so on) into useful high grade heat. But, for the development such systems, the first and foremost requirement is the selection of best suited working pair with the prediction of system performance. Therefore, in the present study, authors have investigated the performance of MHHT employing the metal hydride pair of La_{0.9}Ce_{0.1}Ni₅ and LaNi_{4.6}Al_{0.4}. The pair of La_{0.9}Ce_{0.1}Ni₅ and LaNi_{4.6}Al_{0.4} hydrides are chosen based on author's previous study¹ on thermodynamic simulation of MHHT using static and dynamic property data of metal hydrides. In the present study, the performance of MHHT is predicted using UDFs in ANSYS Fluent. It is to be noted that very few studies have been carried out in past on the performance analysis of metal hydride based thermal systems in ANSYS Fluent. It is also observed from the literature that such a performance analysis not been conducted for the chosen MH pair. This study could provide a basis for further studies by introducing a new perspective.

2 | WORKING PRINCIPLE OF MHHT

It is typical a metal hydride based thermodynamic application. The purpose is to consume industrial and/or other sources of waste heat and upgrade it to useful thermal energy that can be again utilized by industries or other high temperature applications. Due to its efficiency, flexible temperature range, and safe operation without any moving parts, this application is particularly attractive. The thermodynamic cycle of a single stage MHHT represented in van't Hoff plot is shown in Figure 1. The working cycle consists of two combined forms of heat and mass exchange processes, that is, heat transformation (A-B) and regeneration (C-D) processes and two sensible heat exchange processes, that is, sensible heating (C-B and D-A) and sensible cooling (A-D and B-C). The framework operates within three temperature limits, that is, heat output temperature (T_H), driving heat temperature (T_M), and heat sink temperature (T_L) and two pressure limits ($P_H > P_L$). The heat transformation and regeneration processes are hydrogen transfer processes in

FIGURE 1 General van't Hoff representation of MHHT cycle. MHHT, metal hydride based heat transformer

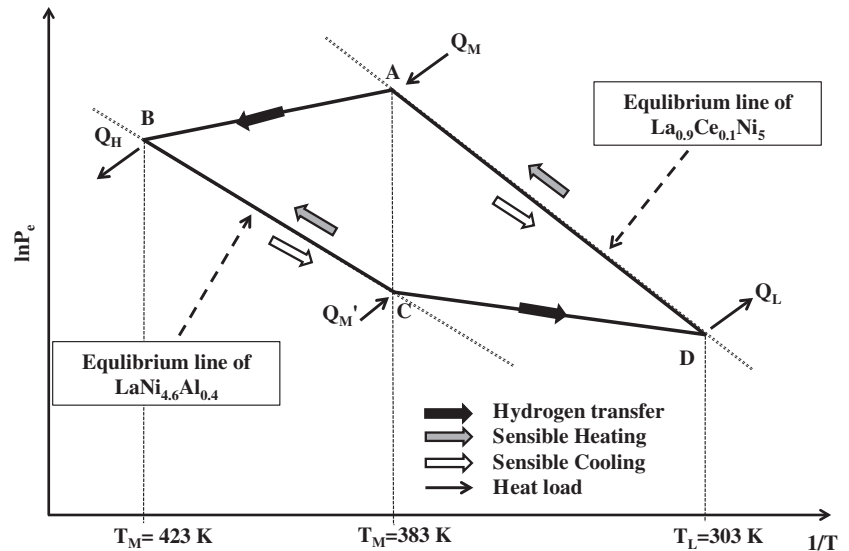


TABLE 1 Properties of metal hydrides^{18,19}

Metal hydride	Reaction enthalpy; ΔH (kJ/mol)	Reaction entropy; ΔS (J/mol K)	Activation Energy; ΔE (kJ/mol)	Slope factor; $\Phi + \Phi_0$	Hysteresis factor; β	
LaNi _{4.6} Al _{0.4}	34.04	108	30.51	30.89	1.40 ± 0.01	0.45
La _{0.9} Ce _{0.1} Ni ₅	25.98	104	28.54	28.26	0.45 ± 0.01	0.45

which the reaction enthalpies are considered as heat loads (heat effects) whereas sensible cooling and heating of the reactor are done externally through heat transfer fluid to change the thermodynamic states of the reactors (MH beds) for next half-cycle.

In the beginning, it is made sure that MH bed A is completely hydrogenated and MH bed B is completely dehydrogenated and maintained at their respective working temperatures viz., T_M and T_H . MH bed A starts to desorb hydrogen by taking heat (Q_M) at T_M (endothermic reaction) and MH bed B starts to absorb that hydrogen by releasing the heat (Q_H) at T_H (exothermic reaction). Here, Q_H is the useful upgraded heat form Q_M . This procedure is carried out until a complete transfer of hydrogen happens between beds A and B. Simultaneously, for regeneration, the MH bed C starts to desorb hydrogen by isolating the heat (Q_M') from the driving heat temperature T_M and the MH bed D starts to absorb the hydrogen by rejecting heat (Q_L) at low temperature T_L . This is continued until the proportion of hydrogen trade between reactors C and D is completed, that is, till equilibrium between the reactors is established. After completion of heat transformation and regeneration processes, the hydrogen transfer valves are closed and heat transfer fluid is circulated in the annulus of reactors for sensible heating and cooling processes. MH beds A and B are sensibly cooled from T_M to T_L and T_H to T_M , respectively, whereas MH beds C and D are sensibly heated from T_M to

T_H and T_L to T_M , respectively. Upon sensible heating and cooling, MH beds interchanged their thermodynamic states and ready for next half-cycle.

As already mentioned that the metal hydride pair, that is, La_{0.9}Ce_{0.1}Ni₅ and LaNi_{4.6}Al_{0.4} is chosen based on our previous work.¹⁸ The desired properties of metal hydrides suitable for MHHT are high hydrogen storage capacities that increases hydrogen transmission, fast reaction kinetics to reduce overall cycle time, flatter $\alpha + \beta$ phase and low hysteresis, facilitating higher mass flow rates between metal hydride beds due to high pressure difference at fixed operating temperatures, and favorable thermodynamic properties, that is, high absorption enthalpy of MH responsible for heat transformation (B and C) and low desorption enthalpy of MH working for regeneration (A and D). The required metal hydride properties for present study are listed in Table 1.

3 | COMPUTATIONAL METHODOLOGY

The mathematical modeling of MHHT with alloys pair of La_{0.9}Ce_{0.1}Ni₅-LaNi_{4.6}Al_{0.4} is carried out to study the behavior of MH beds in terms of bed temperature and hydrogen concentration. For simulation of complete process, discretization of governing equations for mass and energy

balance are done, which converts the differential form of governing equations into set of algebraic equations.

3.1 | Assumptions

1. The local thermal equilibrium exists between metal hydride bed and hydrogen gas.
2. Heat transfer through radiation within metal hydride is neglected.
3. Hydrogen is considered as ideal gas.
4. Effect of hydrogen concentration on thermo-physical properties of metal hydride is neglected.
5. Heat transfer from reactor to surrounding is neglected.

The equilibrium pressure of MH beds state can be determined by van't Hoff equation (Equation 1).

$$P_{eq} = 10^5 \exp \left[\frac{\Delta H}{R_u T} - \frac{\Delta S}{R_u} + (\varphi \pm \varphi_0) \tan \left[\pi \left(\frac{x}{x_f} - \frac{1}{2} \right) \right] \pm \frac{\beta}{2} \right] \quad (1)$$

The amount of hydrogen desorbed from desorbing material and absorbed by absorbing material are estimated using following equations:

$$m_d = R_d \exp \left(\frac{-E_d}{R_u T_d} \right) \left(\frac{P_{eq,d} - P_{g,t+\delta t}}{P_{eq,d}} \right) \rho_{m,d} \quad (2)$$

$$m_a = R_a \exp \left(\frac{-E_a}{R_u T_a} \right) \ln \left(\frac{P_{g,t+\delta t}}{P_{eq,a}} \right) (\rho_{SS} - \rho_{m,a}) \quad (3)$$

The temperature variation within the metal hydride beds during hydrogen transfer processes can be calculated from following energy equation.

$$(\rho C_p)_e \frac{\partial T}{\partial t} + (\rho C_p)_g \vec{u} \cdot \nabla T = \lambda_e \nabla^2 T - m_d \left[\frac{\Delta H}{M_g} - T(C_{p,g} - C_{p,m}) \right] \quad (4)$$

The detailed step-wise methodology for solving above equations and boundary conditions are available in author's previous article.⁶

The MHHT required four MH beds for simultaneous operation of heat transformation and regeneration processes, that is, heat transformation operates between $\text{La}_{0.9}\text{Ce}_{0.1}\text{Ni}_5$ (A) and $\text{LaNi}_{4.6}\text{Al}_{0.4}$ (B) whereas regeneration operates between $\text{LaNi}_{4.6}\text{Al}_{0.4}$ (C) and $\text{La}_{0.9}\text{Ce}_{0.1}\text{Ni}_5$ (D). The analysis model is prepared in ANSYS using dimensions presented by Satya Sekhar and Muthukumar⁹ as shown in Figure 2, the model shows four beds, which depict the two above stated processes amongst two complementary pair. The reactors have an outer diameter of 32 mm and an inner diameter of 12 mm. Each reactor bed has a length of 500 mm.

For the model, a standard mapped face meshing (as shown in Figures 3 and 4) is introduced throughout the model with all default initializers. Moreover, each cylinder is employed upon with a sweep method with quad/tri mesh incorporating five divisions.

In the present study, numerical model is used through user-defined functions (UDFs) in ANSYS, the UDFs include the various material properties and required constants corresponding to Equations (1-3). The detailed numerical modeling is presented elsewhere⁶ and the boundary temperature conditions are patched

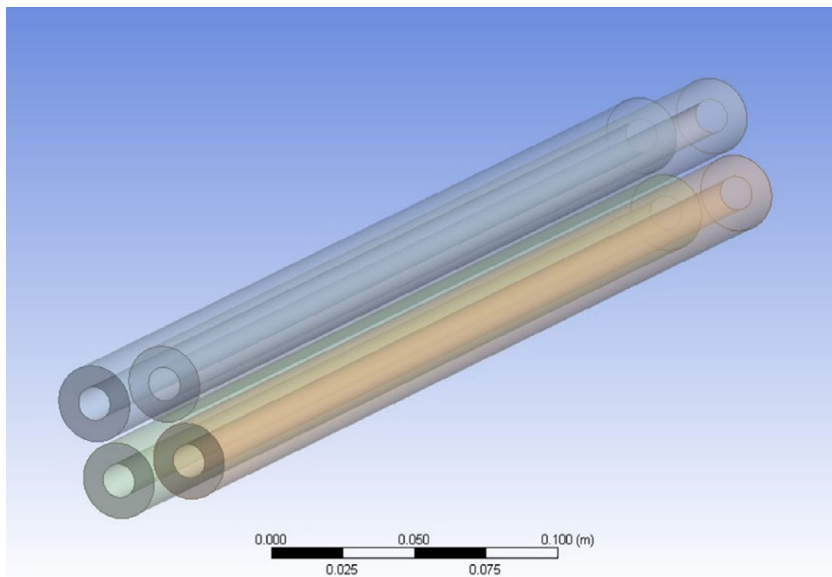


FIGURE 2 Reactor geometry

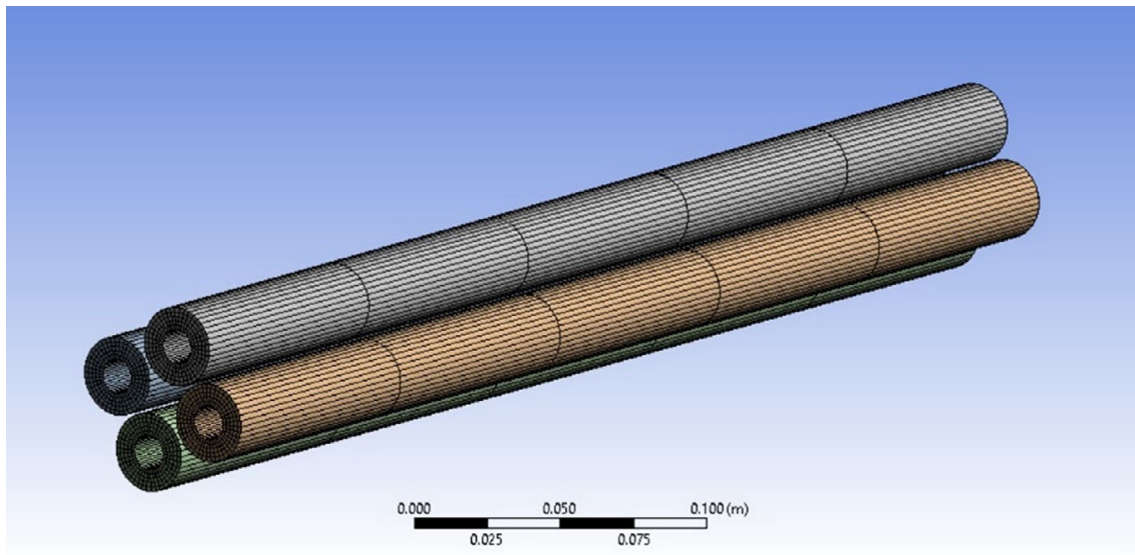


FIGURE 3 Meshing (full body view)

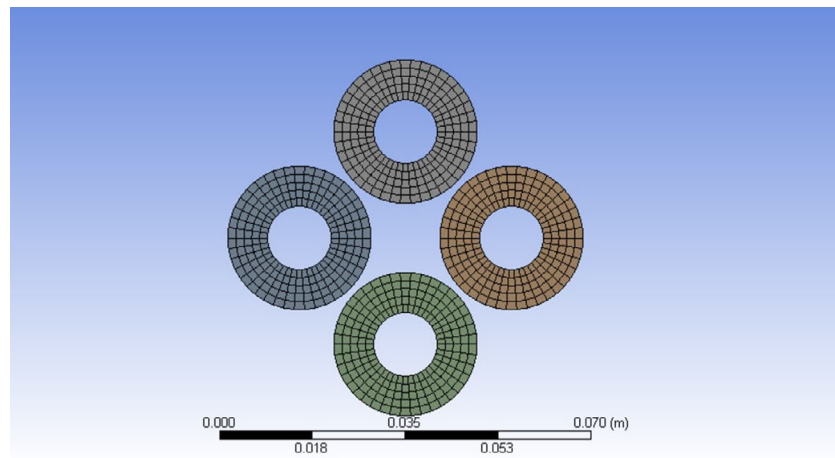


FIGURE 4 Meshing (front view)

for each cylinder. With hybrid initialization of the problem, results are derived.

4 | RESULTS AND DISCUSSION

4.1 | Temperature contours during hydrogen transfer processes

The thermal behavior of the system through temperature variation of metal hydride bed has been analyzed through ANSYS Fluent 16. The user-defined functions are incorporated in the CFD simulation software ANSYS Fluent to solve the governing equations for mass, equilibrium pressure and energy. The iterative values of temperature during each time step has been solved by user-defined functions and represented with the help of contours generated through ANSYS. The contours presented in Figures 5–8 show the variation of temperature for all four reactors. The cut

section at the mid of axial length and perpendicular to the axis of reactor has been taken to represent the temperature of reactor at any instance throughout the analysis. Figure 5 shows the temperature of the reactor at beginning ($t = 0$ second), when the reaction is about to start. It is clear from the contours of Figure 5 that initially reactor B is kept at highest temperature of system, that is, 423 K, reactors A and C maintained at 383 K, while the reactor D is maintained lowest temperature 303 K. In the present study contours, the interaction between metal hydride beds A and B show the process of useful heat generation and the interaction between metal hydride beds C and D show the regeneration process.

As discussed previously the heat transformation by the reactor B at temperature (T_H) is achieved during the hydrogen transfer between the reactors A and B for first half-cycle of the system. The Figure 6 shows the contours of maximum temperature value, that is, 473 K for reactor B at first 85 seconds during heat transformation process. The maximum attained temperatures of the other

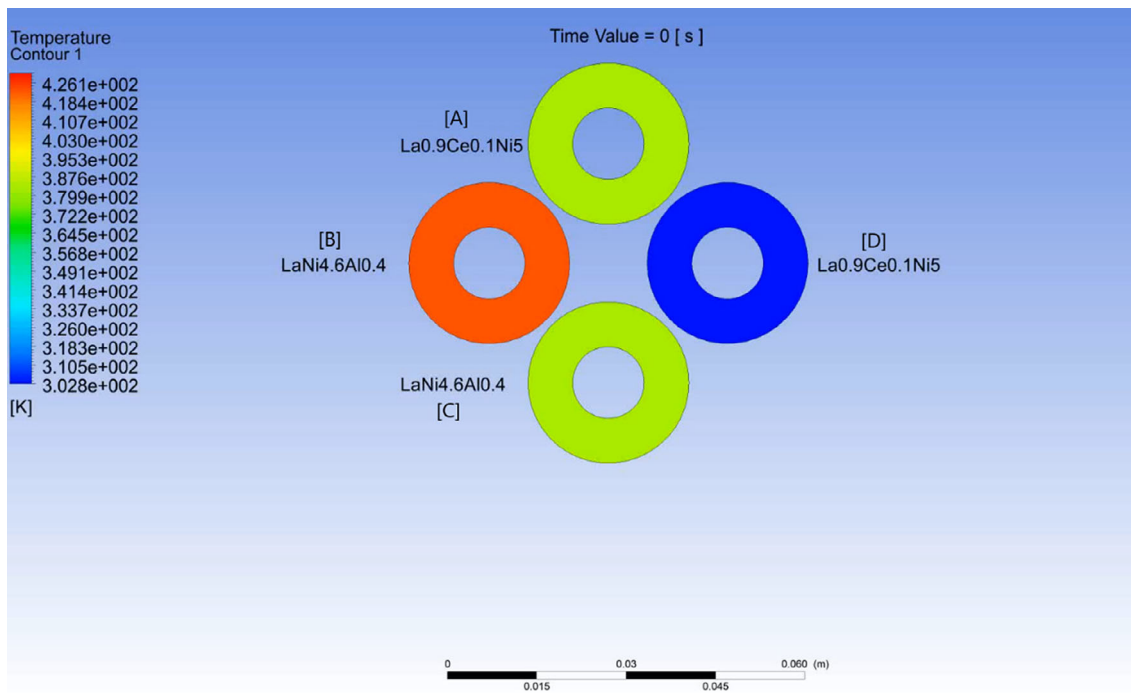


FIGURE 5 Initialization of hydrogen transfer processes

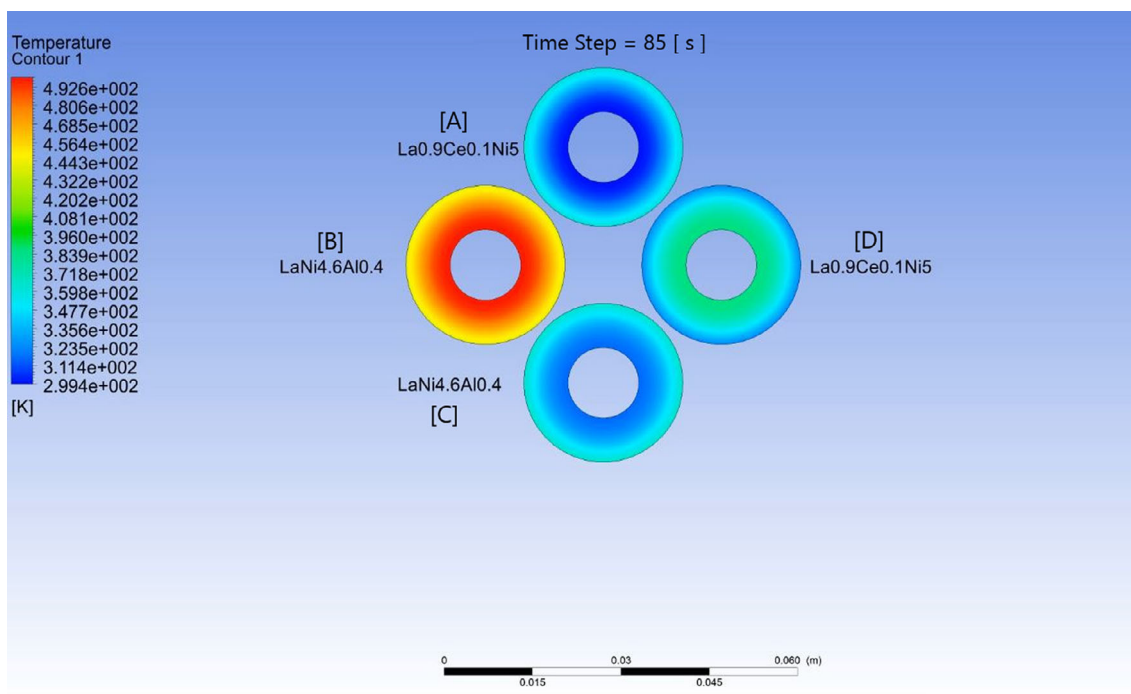


FIGURE 6 Transition stage at 85 seconds of hydrogen transfer processes

reactors with their respective time are available in Table 2. The contour of reactor B, in Figure 6, shows the effect of convective cooling through water jacket at outer periphery of the reactor, due to which the outer radius of the reactor B shows lower temperature compare to its inner radius. Similarly, at 85 seconds, other two desorbing reactors A and C show higher temperature at outer

radius while reactor D shows higher temperature at its inner radius due to exothermic reaction propagating from inner to outer radial direction.

Figure 7 shows the contours for temperature of all the reactors at the end of the hydrogen transfer process at 880 seconds. As the hydrogen transfer finished, the immediate effect of sensible

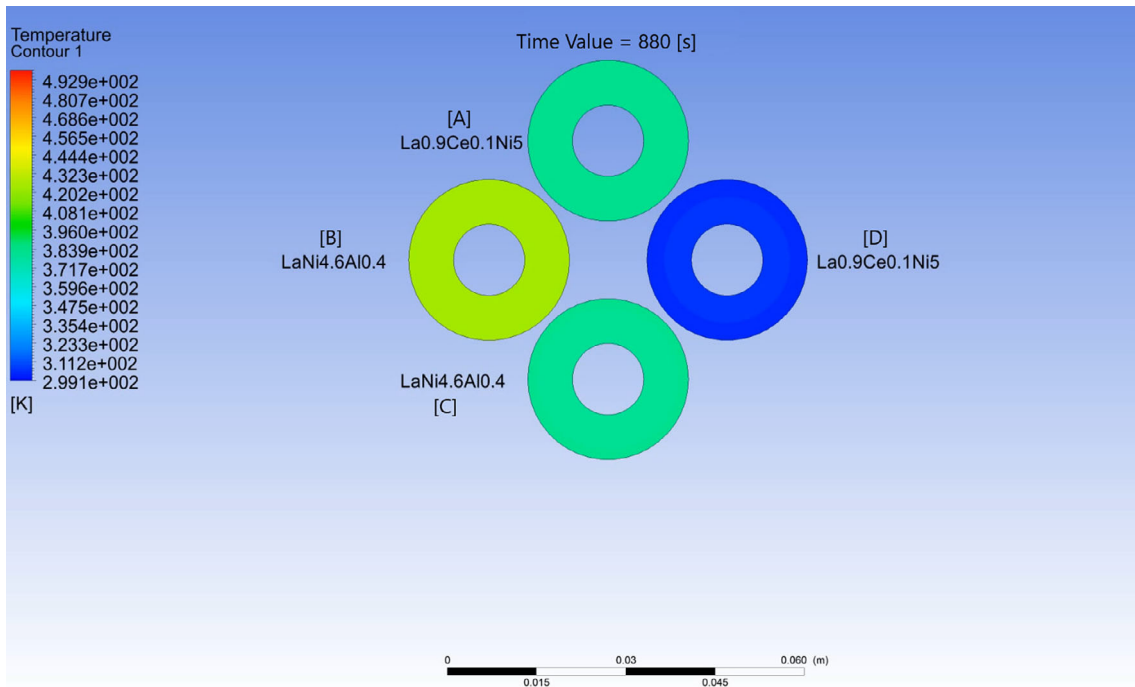


FIGURE 7 End of hydrogen transfer processes

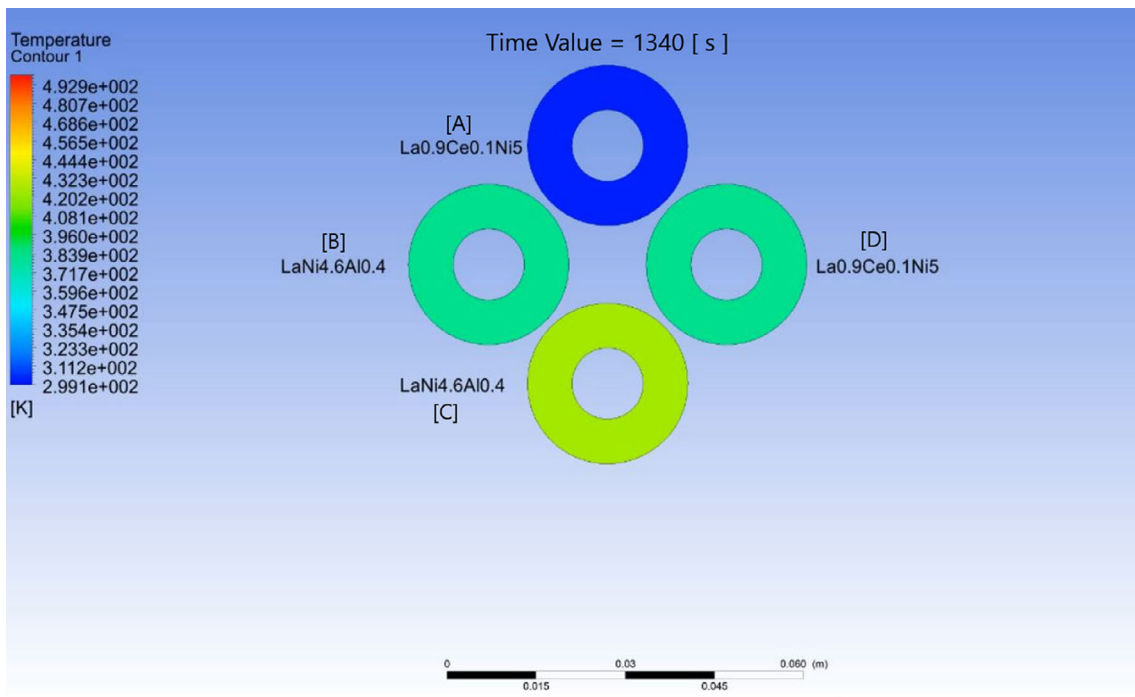


FIGURE 8 End of sensible heat transfer processes

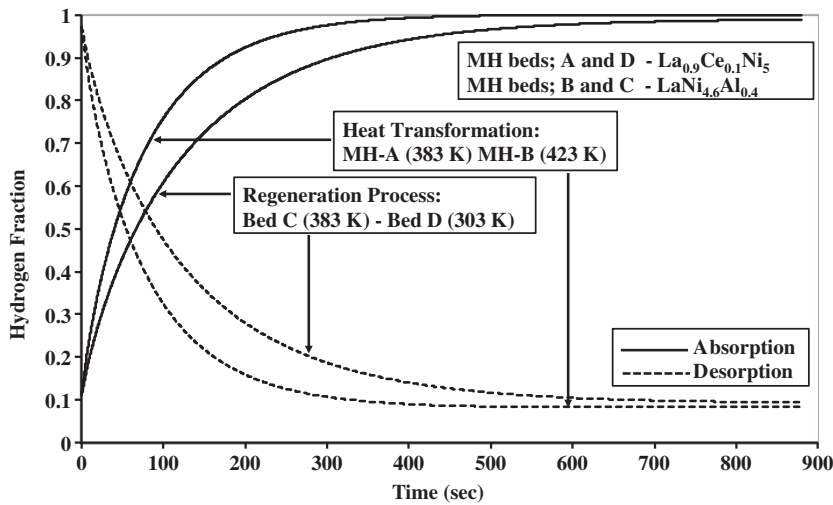
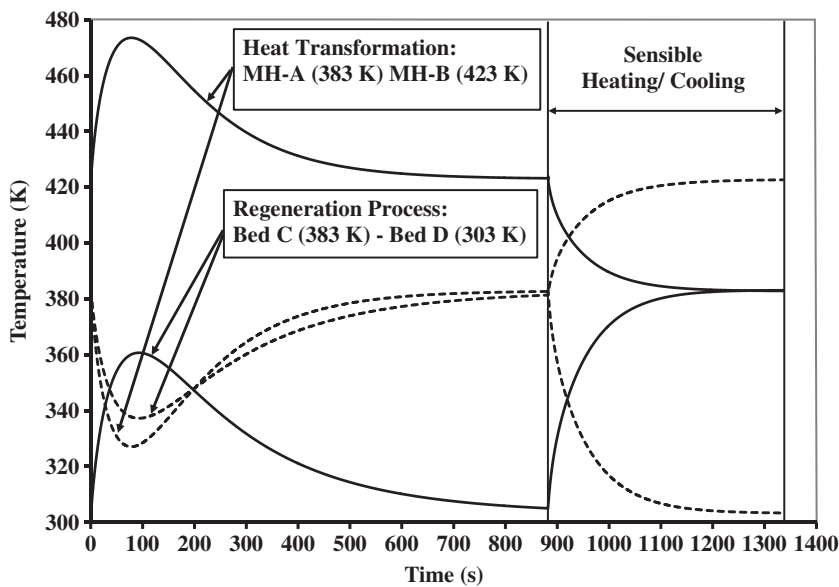
heat transfer takes place for all the reactors. The temperature variations taking place for all the reactors during hydrogen transfer diminished towards completion of the sensible heat transfer process and at the end of the sensible heat transfer processes counters of temperature for all reactors can be referred as required temperatures of reactors for next half-cycle as shown in Figure 8.

4.2 | Hydrogen concentration

The coupled hydrogen transfer between all the paired reactors corresponds to heat transformation and regeneration processes are presented in Figure 9. The hydrogen transfer processes for entire cycle are modeled in such a way that there should be a

TABLE 2 Rise and drop in MH bed temperature during hydrogen transfer processes

Sr. no.	Metal hydride pairs desorbing bed—absorbing bed	Process	Drop in temperature of desorbing bed	Rise in temperature of absorbing bed
1	La _{0.9} Ce _{0.1} Ni ₅ (A)-LaNi _{4.6} Al _{0.4} (B)	Heat Transformation	From 383 K to 327 K in 85 s	From 423 K to 473 K in 85 s
2	LaNi _{4.6} Al _{0.4} (C)-La _{0.9} Ce _{0.1} Ni ₅ (D)	Regeneration	From 383 K to 337 K in 95 s	From 303 K to 360 K in 93 s

**FIGURE 9** Variation of hydrogen concentration**FIGURE 10** Average bed temperature variation

sufficient pressure difference exists between coupled reactors to reduce the overall cycle time. The overall time taken for hydrogenation and dehydrogenation during all the hydrogen transfer processes is 880 seconds. Figure 9 shows the hydrogen transfer for heat transformation as well as regeneration process. Since, all the hydrogen transfers are occurring simultaneously, the rate of mass fractions transfer between all the paired reactors are plotted in a same time span of 0 to 880 seconds.

4.3 | Average bed temperature

Figure 10 shows the thermal behavior of metal hydride reactors during heat transformation as well as regeneration

process. The heat transformation effect, that is, Q_H , from MHHT system is possible immediate after hydrogen absorption by MH bed B at 423 K, which is desorbed by MH bed A (Figure 10) at 383 K. At the same time, regeneration process between reactor C and D is also taking place at 383 and 303 K respectively. When the hydrogen transfer start from reactor A, which is at 383 K results sudden drop in MH bed temperature that can be seen in Figure 10. Similarly, the temperature variations for other absorbing as well as desorbing MH beds are also available in Figure 10. Due to difference in reaction rate and poor thermal conductivity of different metal hydride bed, there will be a variation in time

to attain the maximum and minimum temperature during hydrogen transfer processes, which is available in Table 2.

It can be seen from Figure 10 that the temperature of $\text{La}_{0.9}\text{Ce}_{0.1}\text{Ni}_5$ (A) rapidly falls down to 327 K from 383 K within 85 seconds of hydrogen transfer process during heat transformation process between $\text{La}_{0.9}\text{Ce}_{0.1}\text{Ni}_5$ (A) and $\text{LaNi}_{4.6}\text{Al}_{0.4}$ (B). Similarly, the drop in temperature of $\text{LaNi}_{4.6}\text{Al}_{0.4}$ (C) from 383 to 337 K within 95 seconds during regeneration process between $\text{LaNi}_{4.6}\text{Al}_{0.4}$ (C) and $\text{La}_{0.9}\text{Ce}_{0.1}\text{Ni}_5$ (D) can be seen. These drops in temperatures can be efficiently used for heating applications through heat transfer fluid. It is also observed that the maximum rise and minimum drop in beds temperature occur in first 90 seconds for all the MH beds designating the existence of fast reaction kinetics during the inception of hydrogen transfer processes.

Further, the MH beds are sensibly cooled to extract the higher-grade energy produced in the bed B and prepare them for the next process. These are represented by the same curves across time step of 880 seconds, as an exponential decrease in the variation line. Here, the temperature of the beds is brought down to 303 K and 383 K for bed A and bed B, respectively. Similarly, the MH beds C and D are sensibly heated to raise the temperatures to 423 K and 383 K, respectively. This would prepare the two beds for the next cycle of operation and the processes would continue.

The results obtained in the present study are compared with the results measured with a laboratory model by Isselhorst and Groll.²⁰ They developed a two stage MHHT having a capacity of 8 kW with the metal beds $\text{LmNi}_{4.85}\text{Sn}_{0.15}$, $\text{LmNi}_{4.49}\text{Co}_{0.1}\text{Mn}_{0.205}\text{Al}_{0.205}$, and $\text{LmNi}_{4.08}\text{Co}_{0.2}\text{Mn}_{0.62}\text{Al}_{0.1}$. Their study had a sink temperature of 30 to 40°C compared to our sink temperature of 30°C and their model upgraded the heat energy from a temperature of 130 to 140°C to 200°C which means that their thermal energy got upgraded around by 60°C which can be seen matching with our temperature range of 150 to 200°C, a 50°C thermal heat upgrade, their T_H being higher because of two stage MHHT.

Apart from numerical studies on performance prediction of MH beds heat transformation and regeneration processes, thermodynamic analysis of MHHT is carried. The thermodynamic equation used for evaluating COP and heating output is given in author's previous article.¹⁸ The mass of alloy taken as 250 g, transferable amount of hydrogen and cycle time are taken based on above numerical study. The PCI, kinetics, and thermodynamic properties are taken from author's previous article.¹⁸ The Thermodynamic simulation results in following observations: for 250 g of each metal hydrides and hydrogen transfer time of 880 seconds, MHHT produces 40 kJ of upgraded high temperature heat output with heating capacity of 0.1 kW. The COP and specific alloy output are estimated as 0.46 and 93 W/250 g of metal hydride, respectively.

5 | CONCLUSIONS

The presented study is an intense analysis of the performance of metal hydride heat transformer. Through an aggressive study of various works demonstrated by different researchers, $\text{La}_{0.9}\text{Ce}_{0.1}\text{Ni}_5/\text{LaNi}_{4.6}\text{Al}_{0.4}$ pair was chosen as the primary material for the analysis. The study used user-defined functions for enforcing the numerical modeling and performance formulae into the model. Following are the observations derived from present study.

1. The performance of MHHT is predicted through CFD simulation by employing UDFs in ANSYS Fluent and through thermodynamic simulation using pair of $\text{La}_{0.9}\text{Ce}_{0.1}\text{Ni}_5$ - $\text{LaNi}_{4.6}\text{Al}_{0.4}$ metal hydrides.
2. With presented graphical results and contours, the different variations viz., variation in hydrogen concentration within the MH beds and variation in temperature experienced by MH beds during heat transformation and regeneration processes, can be seen and understood perfectly.
3. The numerical study results in overall cycle time of 1340 seconds (including sensible heating and cooling processes) along with the temperature ranges over which desired heating effect can be derived. A rise of 50°C in MH bed temperature is observed during heat transformation process.
4. The MHHT produces 40 kJ of upgraded heat with 0.46 COP in 880 seconds of hydrogen transfer time for 250 g of each metal hydride.
5. The derived results showed the working paradigm of the device between the presented temperature ranges.
6. This study is presented in hopes to secure a new base for further extensive studies to be performed upon and ensure the practical utility of such device in the near future.

NOMENCLATURE

$C_{p,g}$	specific heat of gas, kJ/kg K
$C_{p,m}$	specific heat of metal hydride, kJ/kg K
K	temperature in Kelvin
M_g	Molecular weight of hydrogen, kg/kmol
m	MASS flow rate of hydrogen, kg/m ³ s
P_H	higher pressure limit
P_L	lower pressure limit
P_{eq}	hydride equilibrium temperature, bar
P_g	hydrogen gas pressure, bar
Q_H	heat load at output temperature, kJ
Q_M	heat load at driving temperature, kJ
Q_L	heat load at sink temperature, kJ
R	reaction rate constant, s ⁻¹
R_u	universal gas constant, kJ/mol K
s	time in seconds
T	temperature

T_H	output heat temperature
T_M	driving heat temperature
T_L	sink temperature
t	time
u	velocity, m/s
x	concentration of hydrogen at the given time (t)
ΔH	enthalpy of reaction, kJ/mol H_2
ΔS	entropy of reaction, J/mol K
ΔE	Activation energy, kJ/mol
ρ_m	density of metal hydride at any time (t)
ρ_{SS}	Saturation density of metal hydride

Subscripts

a	absorption
d	desorption
e	effective
f	final
g	gas

Symbols

$\alpha + \beta$	plateau of PCI
β	hysteresis factor
λ	thermal conductivity, W/m K
$\phi + \phi_o$	slope factors

Abbreviations

COP	coefficient of performance
MH	metal hydride
MHHT	metal hydride heat transformer
PCI	pressure concentration isotherm
SS-MHHT	single stage metal hydride heat transformer
TS-MHHT	two stage metal hydride heat transformer
UDF	user-defined function(s)

ORCID

Vinod Kumar Sharma  <https://orcid.org/0000-0002-5203-1218>

REFERENCES

- Vinod Kumar S, Anil Kumar E. Thermodynamic simulation of hydrogen based solid sorption heat transformer. *Int J Thermal Sci.* 2018;125:74-80.
- Vinod Kumar S, Anil Kumar E. Metal hydrides for energy applications – classification, PCI characterisation and simulation. *Int J Energy Res.* 2017;41:901-923.
- Balakumar M, Murthy SS, Krishna Murthy MV, Sastri MVC. A comparative thermodynamic study of metal hydride heat transformers and heat pumps. *J Heat Recov Sys.* 1985;5:527-534.
- Sun DW, Groll M, Werner R. Selection of alloys and their influence on the operational characteristics of a two-stage metal hydride heat transformer. *Heat Recov Sys CHP.* 1992;12:49-55.
- Ram Gopal M, Murthy SS. Prediction of metal hydride heat transformer performance based on heat transfer and reaction kinetics. *Ind Eng Chem Res.* 1995;34:2305-2313.
- Mohan M, Sharma M, Vinod Kumar S, Anil Kumar E, Satheesh A, Muthukumar P. Performance analysis of metal hydride based simultaneous cooling and heat transformation system. *Int J Hydrogen Energy.* 2019;44:10906-10915.
- Yang FS, Zhang ZX, Wang GX, Bao ZW, Diniz da Costa JC, Rudolph V. Numerical study of a metal hydride heat transformer for low-grade heat recovery: simulation of a MH heat transformer. *Appl Therm Eng.* 2011;31:2749-2756.
- Yang FS, Zhang ZX, Bao ZW. An extensive parametric analysis on the performance of a single-stage metal hydride heat transformer. *Int J Hydrogen Energy.* 2012;37:2623-2634.
- Satya Sekhar B, Muthukumar P. Performance analysis of a metal hydride based heat transformer. *Int Energy J.* 2012;13:29-44.
- Satya Sekhar B, Pailwan SP, Muthukumar P. Studies on metal hydride based single-stage heat transformer. *Int J Hydrogen Energy.* 2013;38:7178-7187.
- Satya Sekhar B, Muthukumar P. Performance investigation of a single-stage metal hydride heat transformer. *Int J Green Energy.* 2016;13:102-109.
- Byung HK, Akira Y. Performance analysis of a metal-hydride heat transformer for waste heat recovery. *Appl Therm Eng.* 1996;16:677-690.
- Kuznetsov AV. Investigation of working cycle of a metal hydride heat transformer for upgrading waste heat. *J Power Energy.* 1996; 210:157-163.
- Werner R, Groll M. Two-stage metal hydride heat transformer laboratory model: results of reaction bed tests. *J Less Common Metals.* 1991;172-174:1122-1129.
- Willers E, Groll M. The two-stage metal hydride heat transformer. *Int J Hydrogen Energy.* 1999;24:269-276.
- Satya Sekhar B, Muthukumar P. Performance tests on a double-stage metal hydride based heat transformer. *Int J Hydrogen Energy.* 2013;38:15428-15437.
- Satya Sekhar B, Muthukumar P. Thermal modeling and performance investigation of a double-stage metal hydride-based heat transformer. *Num Heat Transfer, Part A: Appl.* 2015;67:883-901.
- Vinod Kumar S, Anil Kumar E. Measurement and analysis of reaction kinetics of La-based hydride pairs suitable for metal hydride-based cooling systems. *Int J Hydrogen Energy.* 2014;39: 19156-19168.
- Vinod Kumar S, Anil Kumar E. Studies on La based intermetallic hydrides to determine their suitability in metal hydride based cooling systems. *Intermetallics.* 2015;57:60-67.
- Isselhorst A, Groll M. Two-stage metal hydride heat transformer laboratory model. *J Alloys Compd.* 1995;231:888-894.

How to cite this article: Choudhari M, Ahuja K, Thakkur S, Bardhan S, Sharma VK. Performance investigation of metal hydride based heat transformer. *Energy Storage.* 2019;1:e56. <https://doi.org/10.1002/est2.56>